

## Article

# Nutrient Recovery from Zeolite and Biochar Columns: The Case Study of Marineo (Italy) Wastewater Treatment Plant

Pedro Tomas Bulacio Fischer <sup>1,\*</sup>, Daniele Di Trapani <sup>2</sup>, Vito Armando Laudicina <sup>1,3</sup>, Sofia Maria Muscarella <sup>1</sup>  
and Giorgio Mannina <sup>2</sup>

<sup>1</sup> Department of Agricultural, Food and Forest Sciences, University of Palermo, Viale delle Scienze ed. 4, 90128 Palermo, Italy; vitoarmando.laudicina@unipa.it (V.A.L.); sofiamaria.muscarella@unipa.it (S.M.M.)

<sup>2</sup> Engineering Department, University of Palermo, Viale delle Scienze ed. 8, 90128 Palermo, Italy; daniele.ditrapani@unipa.it (D.D.T.); giorgio.mannina@unipa.it (G.M.)

<sup>3</sup> National Biodiversity Future Center (NBFC), 90133 Palermo, Italy

\* Correspondence: pedrotomas.bulaciofischer@unipa.it

**Abstract:** Rapid population and economic growth have increased the demand for depleting resources. Nitrogen (N) and phosphorus (P) are mineral elements that perform important functions in plants, but their extraction is not sustainable. In addition, these elements contribute significantly to the eutrophication of water bodies. The recovery of these nutrients from wastewater by adsorption techniques offers a promising solution. Previous studies have demonstrated the adsorption capabilities of materials such as zeolite for ammonium ( $\text{NH}_4^+$ ) and biochar for P. In addition, these materials can serve as a source of N and P for plants in a circular economy context. In this regard, this study aims to evaluate the recovery of N and P by the adsorption capacities of zeolite and biochar through a column test with treated wastewater. Two columns positioned in series, one filled with 2.7 kg of zeolite and the other with 397 g of biochar, were placed at the outlet of the full-scale sewage treatment plant of Marineo (Italy). The zeolite adsorbed 3.6 g of  $\text{NH}_4^+$  accumulated during the test with a rate of adsorption of 44% and adsorption of  $1.33 \text{ mg g}^{-1}$  of  $\text{NH}_4^+$ . The biochar adsorbed about 11 g of P accumulated during the test, with an adsorption percentage of 13% and an adsorption of  $26.75 \text{ mg g}^{-1}$  of P. Despite some problems related to the effluent used during the test, the tested materials showed good adsorption properties.

**Keywords:** ammonium; biochar adsorption; circular economy; phosphorus; treated wastewater zeolite adsorption



Academic Editors: Bing Wang,  
Masud Hassan and Yung-Tse Hung

Received: 29 January 2025

Revised: 11 March 2025

Accepted: 13 March 2025

Published: 16 March 2025

**Citation:** Bulacio Fischer, P.T.; Di Trapani, D.; Laudicina, V.A.; Muscarella, S.M.; Mannina, G. Nutrient Recovery from Zeolite and Biochar Columns: The Case Study of Marineo (Italy) Wastewater Treatment Plant. *Water* **2025**, *17*, 848. <https://doi.org/10.3390/w17060848>

**Copyright:** © 2025 by the authors. Licensee MDPI, Basel, Switzerland. This article is an open access article distributed under the terms and conditions of the Creative Commons Attribution (CC BY) license (<https://creativecommons.org/licenses/by/4.0/>).

## 1. Introduction

Ensuring food and nutrition security while preserving natural resources and maintaining environmental quality is one of the greatest challenges of the 21st century [1]. As the human population continues to grow, increasing crop production without a negative environmental impact is the main challenge agriculture faces [2,3]. The rapid increase in the human population leads to an increasing demand for food and water, resulting in increased energy consumption and synthetic fertilizers to improve yields [4]. Together with other chemical elements, nitrogen (N) and phosphorus (P) are macronutrients essential for plants [5,6]. Specifically, N performs several fundamental functions, including protein synthesis, chlorophyll composition, and growth regulation, and it is involved in energy metabolism. P is crucial for energy transfer, nucleic acid synthesis, cell membrane formation, metabolism, root development, and plant reproduction [7–9]. In the agricultural sector, the current production of fertilizers is mainly based on using a large amount of

energy and no renewable resources [10–12]. N for fertilizer production is virtually unlimited through industrial processes such as the Haber–Bosch method, which converts gaseous N to ammonium ( $\text{NH}_4^+$ ), but  $\text{NH}_4^+$  synthesis is energy-intensive. This is because breaking the strong triple bond of molecular N ( $\text{N}\equiv\text{N}$ ) requires considerable energy [13]. In contrast, although reformed on geological time scales through the global biogeochemical cycle, P comes mainly from phosphate rock, a nonrenewable resource. Its extraction rate far exceeds its natural formation, making it a critical factor in global food security. A study of P reserves, which currently exists, estimates that existing reserves could be depleted by 2315 [14]. In addition, the geographical distribution of phosphate rock deposits, from which P is extracted, is concentrated in a limited number of countries, including China, Morocco, and Jordan [15,16]. This distribution creates significant geopolitical challenges globally [17,18]. In addition to the high cost of fertilizers, their environmental impact is also of concern. When plants do not fully absorb N or P from fertilizers, they can percolate into groundwater or run off into surface water, causing eutrophication. Eutrophication is the over-enrichment of water bodies with nutrients, leading to overgrowth of plant biomass. As this biomass decomposes, it depletes dissolved oxygen, severely degrading water quality and altering the structure and function of aquatic ecosystems. Currently, the main strategies to mitigate eutrophication focus primarily on reducing nutrient loads entering water bodies [19–21]. In addition, N fertilizers, while increasing crop yields, do not improve soil fertility. Disproportionate application of N relative to other essential nutrients can result in soil nutrient depletion [14]. Moreover, in the last years, it has been observed that large amounts of nutrients are contained in wastewater sources, which are now deemed to be a valuable source of nutrients that can enhance the physical and chemical properties of the soil, particularly in terms of N, P, organic matter, and other elements, such as calcium, magnesium, iron, sulfur, chlorine, manganese, etc.

Therefore, nutrient recovery from wastewater could make wastewater treatment sustainable, reduce the costs associated with nutrient removal (e.g., less production of surplus sludge), and provide an excellent source of nutrients for crop growth, yield, and quality, while reducing reliance on synthetic fertilizers [22–24]. Many technologies have been investigated for their effectiveness in nutrient recovery, including traditional methods such as chemical precipitation and adsorption [25–28]. Among the various techniques for nutrient recovery, adsorption stands out due to its rapid processing, ease of control, and minimal resource requirements [29]. Several studies have been conducted in batch mode to demonstrate the adsorption capabilities of materials, such as zeolite and biochar, for  $\text{NH}_4^+$  and P recovery, respectively [30–33].

Zeolite is an aluminosilicate mineral known for its remarkable cation adsorption capacity [34,35]. This capacity stems from the isomorphic substitution process where silicon ions ( $\text{Si}^{4+}$ ) are replaced by aluminum ions ( $\text{Al}^{3+}$ ), resulting in an overall negative charge. Zeolite readily exchanges sodium, potassium, calcium, and magnesium cations to balance these negative charges with  $\text{NH}_4^+$  ions [29,31,36]. The adsorption capacity of zeolites was observed in a study conducted by Ashrafizadeh et al. [37]. This study examined the effects of relevant parameters, such as contact time, pH, and initial  $\text{NH}_4^+$  concentration. The results showed that  $\text{NH}_4^+$  removal by clinoptilolite occurs quickly within the first 15 min of contact time. In addition, the pH affects the removal efficiency of  $\text{NH}_4^+$  as it can affect both the character of exchange ions and clinoptilolite. The removal capacity of clinoptilolite  $\text{NH}_4^+$  increases with the increase in the initial concentration of  $\text{NH}_4^+$ . Another example is the study by Karapinar et al. [38], in which the removal of  $\text{NH}_4^+$  by natural zeolite was studied on a laboratory scale using a mechanically mixed batch system (1000 mL). The zeolite used had an average particle size of 13  $\mu\text{m}$  and was used as an adsorbent to remove  $\text{NH}_4^+$ . A relationship has been established between the adsorption

of  $\text{NH}_4^+$  by zeolite and the ratio of initial  $\text{NH}_4^+$  concentration and dosage of zeolite.  $\text{NH}_4^+$  zeolite adsorption was almost completed within the first 5 min of the adsorption period.

Biochar is a carbon content-rich material obtained by biomass pyrolysis from plant or animal origin, usually waste, at high temperatures (300–800 °C) and under limited oxygen conditions [39]. Biochar mainly consists of aromatic-type carbon and is characterized by a very variable surface area, which can vary up to  $1000 \text{ m}^2 \text{ g}^{-1}$ , low density (up to  $600 \text{ kg m}^{-3}$ ), and high porosity (higher than  $0.083 \text{ cm}^3 \text{ g}^{-1}$ ) [40,41]. Biochar has high total and organic carbon content and holds macroelements (i.e., potassium, sodium, magnesium, calcium, etc.) and microelements (i.e., copper, zinc, iron, etc.) [42,43]. The affinity of biochar for P adsorption is influenced by several factors, including its physical and chemical properties, production conditions, and the characteristics of the soil and wastewater to which it is applied [44–46]. Zhao et al. [47] have tested biochar from different raw materials to test their adsorption capabilities. They observed that different sources of biochar have significantly different phosphate adsorption capabilities. Indeed, using three different types of biochar, they found that pine biochar could adsorb up to  $14 \text{ mg}$  of phosphate  $\text{g}^{-1}$ , while the other two biochars produced from corn straw adsorbed  $9 \text{ mg g}^{-1}$ . Mor et al. [48] conducted a study to evaluate the effect of contact time, adsorbent dose, pH, and temperature on adsorption. Their results showed that activated ash from rice husk provides more efficient and economical removal of phosphate from wastewater. They found that 89% of phosphate removal was achieved at pH 6 using a dose of  $2 \text{ g L}^{-1}$  in 120 min of contact time. Based on the findings of the above-reported studies, zeolite and biochar can be used for N and P adsorption from treated wastewater at full scale. Then, the enriched adsorbents could be used as fertilizers within a circular economy perspective.

This study aims to evaluate the feasibility of using zeolite and biochar for  $\text{NH}_4^+$  and P recovery through column adsorption experiments. Unlike most studies available in the literature, which generally rely on batch adsorption tests with monocomponent synthetic solutions, this research was conducted at full scale using real treated wastewater. For example, one of the few studies performed in the column was carried out by Bulacio Fischer et al. [49]. The authors in this study investigated the  $\text{NH}_4^+$  adsorption capacity of zeolite in columns and the influence of some parameters, such as flow rate and particle size of the material. The authors tested three values of flow rate and two zeolites with different particle diameters. The results showed that the higher flow rate increased the adsorption capacity of both zeolites by about 29% more than the lower flow rate. In addition, the 0.5–1.0 mm zeolite adsorbed about  $60 \text{ mg}$  more  $\text{NH}_4^+$  than the 2.0–5.0 mm zeolite, highlighting the influence of particle size on adsorption capacity. Another study concerning the use of biochar in columns was carried out by Januševicius et al. [50], in which the authors tested the adsorption capabilities of biochar obtained from sewage sludge and at different pyrolysis temperatures. The results showed that the material efficiently removed P from wastewater. The biochar with the best P adsorption was obtained at a pyrolysis temperature of 600 °C with a removal rate of 87%.

Adsorption columns, filled with biochar and zeolite, were fed through a deviation line with treated wastewater from the full-scale wastewater treatment plant (WWTP) in Marineo, Italy, built within the EU project of Achieving Wider-Uptake of Water Smart Solutions [51,52]. The novelty of the present study relies on the use of real treated wastewater from a full-scale WWTP and two-step biochar and zeolite columns at the pilot scale. The results of the experiments coupled with the investigated operational conditions yielded important information enabling an evaluation of the adsorption performance of the selected materials under realistic conditions, taking into account the potential challenges and related issues of operating at a full-scale plant, also facing the complexity of real wastewater

use. Moreover, the results of the present study could provide useful insights in view of treatment scale-up, with potential application of nutrient recovery at full scale.

## 2. Materials and Methods

### 2.1. Description of the Marineo WWTP

The Marineo WWTP was designed to handle a daily flow of  $2160 \text{ m}^3 \text{ day}^{-1}$ , close to 7000 equivalent inhabitants. The treatment process begins with a pretreatment stage, including screening, degritting, primary clarification, and equalization. The plant featured a CAS layout with two identical combined basins operated in parallel, followed by a surface filtration unit. It was characterized by a two-step disinfection stage, as outlined below. In more detail, each combined basin contained an activated sludge reactor with a net volume of  $300 \text{ m}^3$ , a secondary clarifier with a volume of  $200 \text{ m}^3$  and a horizontal surface area of  $540 \text{ m}^2$ , and an aerobic digester with a volume of  $250 \text{ m}^3$ . Each basin was completed by a disinfection unit characterized by the addition of a sodium hypochlorite solution stored in a dedicated tank. The effluent water from the combined basins was then fed to the surface filtration units. After filtration, the treated flow rates were reunited and subject to a UV disinfection stage before discharge. Although an irrigation network was planned, it has not yet been implemented, so the effluent from WWTP is currently discharged into a nearby river. Figure 1 depicts a panoramic view of the Marineo WWTP, while Table 1 summarizes the main quality features of inlet and outlet parameter concentrations (average values) of the Marineo WWTP.

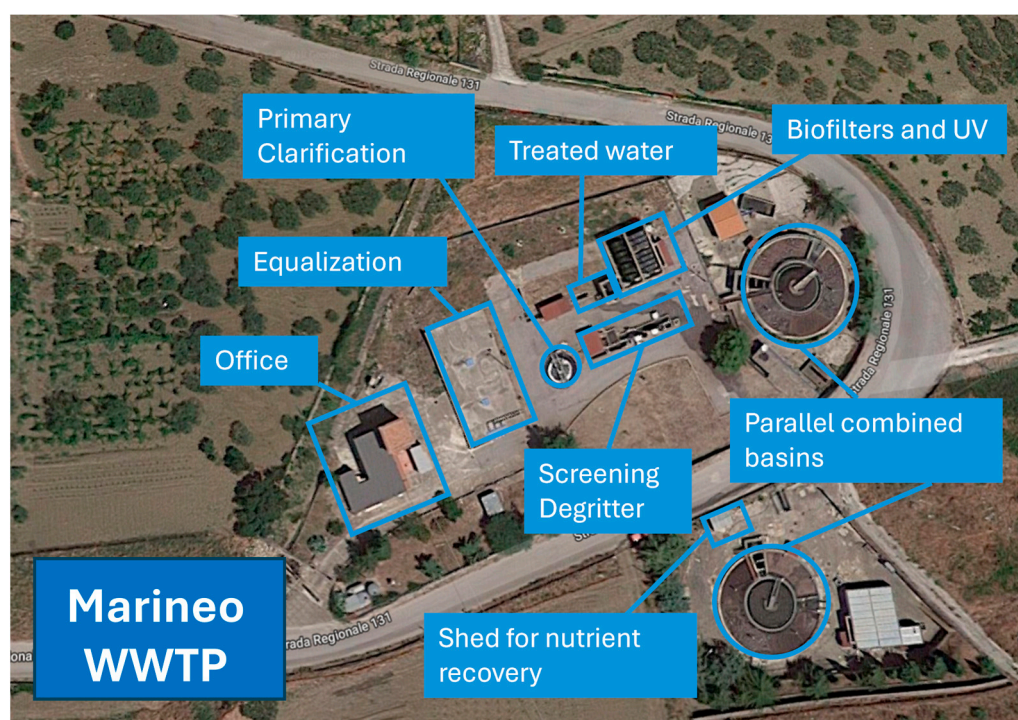


**Figure 1.** Panoramic view of Marineo WWTP (source <https://earth.google.com/web/> accessed on 20 December 2024).

As better outlined below, in the frame of the Wider-Uptake (WU) Project, one aim of the activities carried out at the Marineo WWTP was to demonstrate the feasibility of nutrient recovery from treated wastewater using adsorbent materials. To meet this aim, the construction of a deviation line into a covered location (shed) for the recovery columns was realized [47].

**Table 1.** Inlet and outlet average values of the main quality parameters for the Marineo WWTP.

WWTP Marineo			
Parameter	Units	Influent	Effluent
TSS	[mg L <sup>-1</sup> ]	283	33
pH	-		7.8
BOD <sub>5</sub>	[mg L <sup>-1</sup> ]	278	20
COD	[mg L <sup>-1</sup> ]	566	43
TP	[mg L <sup>-1</sup> ]	13	3
NH <sub>4</sub> <sup>+</sup>	[mg L <sup>-1</sup> ]	24	0.16
NO <sub>2</sub> <sup>-</sup>	[mg L <sup>-1</sup> ]	n.a.	1.03
NO <sub>3</sub> <sup>-</sup>	[mg L <sup>-1</sup> ]	n.a.	18

## 2.2. Biochar and Zeolite Characteristics

The biochar (Nera Biochar s.p.a, Turin, Italy) used in this study to fill the first column was characterized and the characteristics are reported in the Table 2.

**Table 2.** Characteristics of biochar used in this study.

Parameters	Unit	Value
Bulk density	g L <sup>-1</sup>	180
Surface area	m <sup>2</sup> g <sup>-1</sup>	194
Total pore volume	cm <sup>3</sup> g <sup>-1</sup>	38
pH		9.1
Electrical conductivity	dS m <sup>-1</sup>	1.3
Total carbon	%	62
Total limestone	%	5
Total nitrogen	%	0.8
Total sulfur	%	0.1
Fe	mg g <sup>-1</sup>	22
Zn	mg g <sup>-1</sup>	0.0017
Molar ratio H:C		0.7

The second column was filled with zeolite (ZEOWATER ZN, Zeocel Italia, Pisa, Italy). The characteristics of the tested zeolite are reported in Table 3.

**Table 3.** Characteristics of zeolite used in this study.

Parameters	Unit	Value
Bulk density	g cm <sup>-3</sup>	0.98
Surface area	m <sup>2</sup> g <sup>-1</sup>	40
Si/Al ratio		4.8–5.5
pH		7.6
Clinoptilolite	%	85
Cristobalite	%	8
Illite	%	4
Plagioclase	%	3

The biochar and zeolite used in this study were characterized in previous studies [43,52]. The point of zero charge (pHpzc) of the biochar and zeolite used in this study was assessed using the pH drift method, following the procedure outlined by Nasiruddin et al. [53] and described in Vaičiukynienė et al. [54]. A 0.01 M sodium chloride (NaCl) solution was used as the background electrolyte. Eight solutions with pH values ranging from 2 to 9 were prepared by adjusting the pH with small amounts of 0.5 M HCl or 0.5 M NaOH.

Each solution was mixed with 1.0 g of biochar or zeolite and left to equilibrate for 24 h at room temperature. The final pH of each solution was recorded, and the pHPzc was identified as the point where the initial and final pH values were equal, indicating a neutral surface charge [54]. The maximum adsorption capacity of biochar and zeolite tested, was investigated using mono-component solutions. Two grams of biochar was placed in contact with 100 mL of a 1000 mg P L<sup>-1</sup> solution, prepared using dipotassium monohydrogen phosphate (K<sub>2</sub>HPO<sub>4</sub>). The biochar was agitated on a shaker at 80 rpm for 24 h. After the contact period, the biochar was separated from the solution by filtration using Whatman paper 42, washed twice with distilled water (at a 1:2.5 ratio, *w:v*), and subsequently dried at 60 °C for 72 h. To evaluate NH<sub>4</sub><sup>+</sup> adsorption capacity, 1 g of zeolite was mixed with 100 mL of a 20 g NH<sub>4</sub><sup>+</sup> L<sup>-1</sup> solution and shaken on an orbital shaker at 80 rpm for 24 h at 25 °C. Following the incubation period, the sample was washed three times with 200 mL of distilled water to remove excess NH<sub>4</sub><sup>+</sup> and then dried in an oven at 105 °C for 2 h. The amount of NH<sub>4</sub><sup>+</sup> adsorbed by zeolite was determined using Kjeldahl distillation, with 30 mL of 33% (*w/v*) NaOH solution for 6 min [31]. Biochar and zeolite were also analyzed using a PerkinElmer Spectrum Two FTIR spectrometer equipped with an attenuated total reflectance device for acquiring Fourier transform infrared and attenuated total reflectance (ATR-FTIR) spectra. Such spectra were acquired to assess the main functional groups of tested biochar and zeolite. Approximately 1 mg of pulverized material was used to obtain the spectra in the wavenumber range 3600–600 cm<sup>-1</sup>, with a resolution of 4 cm<sup>-1</sup> and 32 scans, according to Sharma et al. [55]. The spectra have been elaborated by using the PerkinElmer Spectrum (Version 10.5.1) software program.

### 2.3. Experimental Setup

As stated above, the study was conducted at the Marineo WWTP and lasted 73 days from May 2022 to July 2022. Two polymethylmethacrylate columns with an inner diameter of 10 cm and a length of 60 cm were used. The first column was filled with 397 g of biochar with a 2.0–5.0 mm diameter and the second was filled with 2.7 kg of zeolite with a 0.5–1.0 mm diameter. The columns were arranged in series, with the biochar column placed first to recover P, followed by the zeolite column to recover NH<sub>4</sub><sup>+</sup> (Figure 2) [56]. The column filled with biochar was placed first due to the filtration capacity of biochar. Additionally, the setup ensured that the biochar was not carried over to the next column, thereby preventing any mixing of materials with zeolite. In contrast, the zeolite tended to mix with the biochar when the order was inverted. A study by Kocatürk et al. [57], which tested different column configurations with zeolite and biochar (in series, in parallel, and as a mixture), demonstrated that when operated in series, the sequence of the adsorbents does not significantly affect P and NH<sub>4</sub><sup>+</sup> adsorption. The treated wastewater exiting the Marineo plant flowed through the columns at a rate of 16.8 L h<sup>-1</sup>. The flow rate was selected based on literature and empty bed contact time trials (EBCT), as this flow rate ensured a contact time of almost 17 min, which was greater than 15 min. This choice aligns with that reported by Canellas-Garriga [58], who assessed the optimal contact time in column systems using clinoptilolite. They concluded that for long-term applications where adsorption capacity and efficiency are priorities, a EBCT longer than 15 min is preferred.

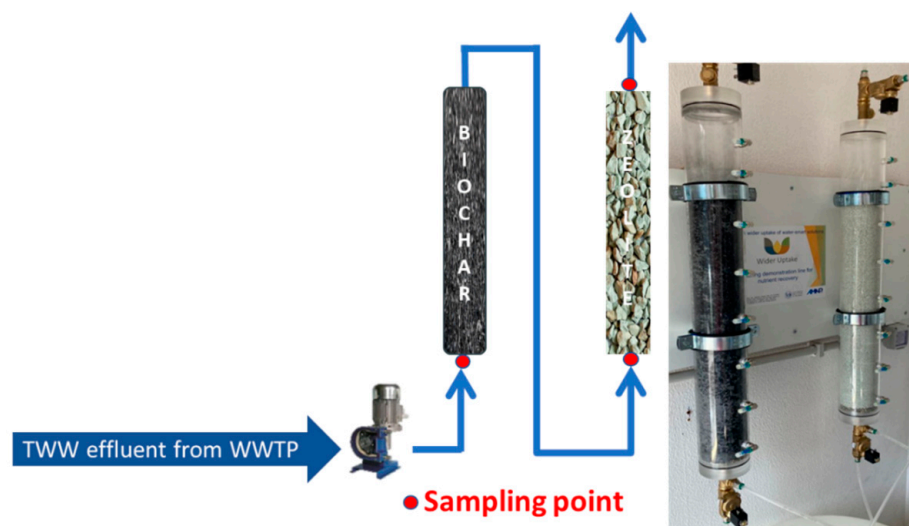


**Figure 2.** Schematic layout and panoramic view of the experimental apparatus.

#### 2.4. Experimental Campaign and Analytical Methods

During the 73-day test period, the water in the inlet and outlet was sampled at least twice a week. Three samples were collected during each sampling time: one at the inlet of the biochar column to monitor the concentration of P and  $\text{NH}_4^+$ , one between the outlet of the biochar column and the inlet of the zeolite column, and one at the outlet of the zeolite column. For each sampling point, 50 mL of water was collected. Once collected, the samples were filtered using 0.45-micron syringe filters to remove impurities and stored in a refrigerator at 4 °C [59]. The samples were analyzed using a spectrophotometer (Thermo Scientific™ GENESYS™ 50 UV-Vis, Waltham, MA, USA) with an analytical kit for P Spectroquant® (Merk KGaA, Darmstadt, Germany) and an analytical kit for  $\text{NH}_4^+$  Spectroquant® (Merk KGaA, Darmstadt, Germany) [49]. After analysis, the mass balance was calculated considering the incoming and outgoing mass and calculating the adsorbed mass by difference. The “in” and “out” mass was calculated by relating the concentration of  $\text{NH}_4^+$  or P in the sample to the product between the flow rate and the system’s hours of operation.

Additionally, approximately 5 g of material was collected periodically during sampling to evaluate the amount of P and  $\text{NH}_4^+$  adsorbed on biochar and zeolite until saturation. The P-enriched biochar samples were pulverized, and the resulting ground materials (0.25 g) underwent mineralization in porcelain crucibles within a muffle furnace at 550 °C for 8 h. The ashes were later recovered through acid digestion using 10 mL of 1 M HCl on a hotplate at 100 °C for 15 min. The digested samples were recovered in 15 mL tubes and adjusted to a volume of 10 mL with MilliQ water. The amount of P was determined by the colorimetric method of Murphy and Riley [60].  $\text{NH}_4^+$  was quantified on 2 M KCl extracts (1:10, *w/v*) through colorimetric analysis employing the Berthelot method [61].

### 3. Results

The  $\text{pH}_{\text{pzc}}$  is a key parameter to determine because it influences the adsorption behavior of materials in aqueous environments by determining their surface charge at different pH levels. In this study, the  $\text{pH}_{\text{pzc}}$  values obtained using the pH drift method were 6.5 for biochar and 6.0 for zeolite (Figure 3).

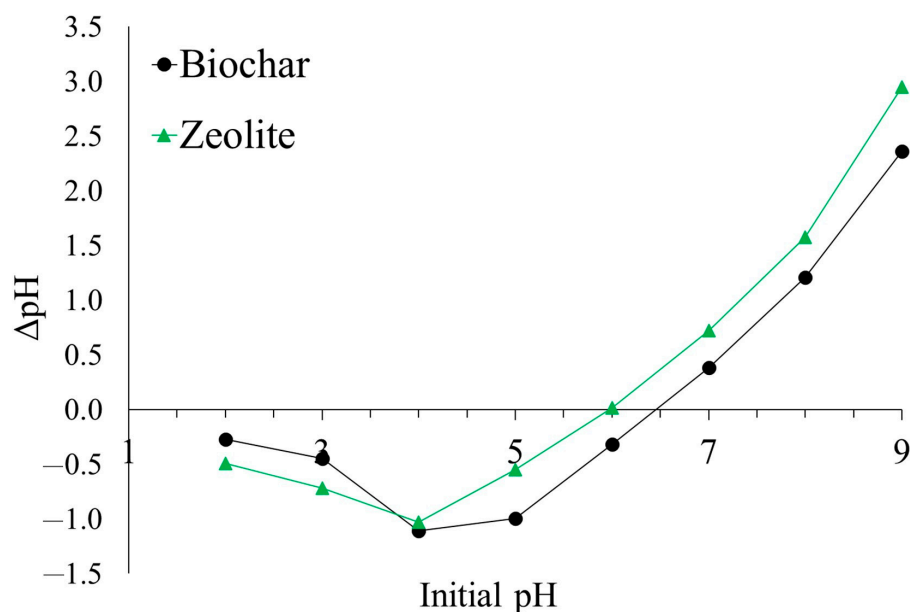


**Figure 3.** Point of zero charge ( $\text{pH}_{\text{pzc}}$ ) of tested biochar and zeolite using the drift method outlined by Nasiruddin et al. [53].

The maximum adsorption capacity of biochar for P in a mono-component solution was relatively low, at  $0.7 \text{ mg P g}^{-1}$ . Zeolite showed a high adsorption capacity for  $\text{NH}_4^+$ , reaching  $29 \text{ mg NH}_4^+ \text{ g}^{-1}$ .

Regarding the analysis of ATR-FTIR spectra, the peaks identified in the ATR-FTIR spectrum of biochar are located at about  $1620 \text{ cm}^{-1}$ ,  $1260 \text{ cm}^{-1}$ , and  $1020 \text{ cm}^{-1}$  (Figure 4a). In contrast, in the analysis of ATR-FTIR spectra, the tested zeolite showed the presence of peaks at  $1650 \text{ cm}^{-1}$ , in the spectral regions of  $1250\text{--}950 \text{ cm}^{-1}$  and  $720\text{--}650 \text{ cm}^{-1}$ , and finally in the range of  $1100\text{--}1000 \text{ cm}^{-1}$  (Figure 4b).

The inlet concentrations of both  $\text{NH}_4^+$  (Figure 5) and P (Figure 6) varied across the sampling days. This variation was more pronounced for  $\text{NH}_4^+$ , with concentrations ranging from  $0.01$  to  $0.35 \text{ mg L}^{-1}$  over several days. In the case of P, the concentration fluctuated between  $1.5 \text{ mg L}^{-1}$  and  $4.0 \text{ mg L}^{-1}$ .

Based on the mass balance analysis, considering the incoming and outgoing mass and calculating the adsorbed mass by difference, it was found that biochar primarily adsorbed P, while zeolite predominantly adsorbed  $\text{NH}_4^+$ . The zeolite was adsorbed with  $1.33 \text{ mg g}^{-1}$  of  $\text{NH}_4^+$ , while the biochar was adsorbed with  $26.75 \text{ mg g}^{-1}$  of P at the end of the trial. For zeolite (Figure 7a), the days of highest  $\text{NH}_4^+$  adsorption were days 3, 37, and 52, with the material adsorbing  $1.3 \text{ g}$ ,  $0.6 \text{ g}$ , and  $1.2 \text{ g}$  of  $\text{NH}_4^+$ , respectively. The highest P adsorption of biochar (Figure 7b) was observed on days 37, 52, and 67, during which it adsorbed  $2.6 \text{ g}$ ,  $3.2 \text{ g}$ , and  $3.3 \text{ g}$  of P, respectively. These peak adsorption days corresponded with the days when the input concentrations to the columns were higher.

Based on the data reported in Figure 8, the zeolite column adsorbed  $3.6 \text{ g}$  of  $\text{NH}_4^+$  at the end of the experiments and the biochar column adsorbed  $10.6 \text{ g}$  of P (Figure 9) throughout the experiments. From the adsorption percentage, calculated by comparing the total mass that circulated in the column to the total mass adsorbed accumulated during the test, it was seen that zeolite had an adsorption percentage of 44% and biochar had an adsorption percentage of 13%.

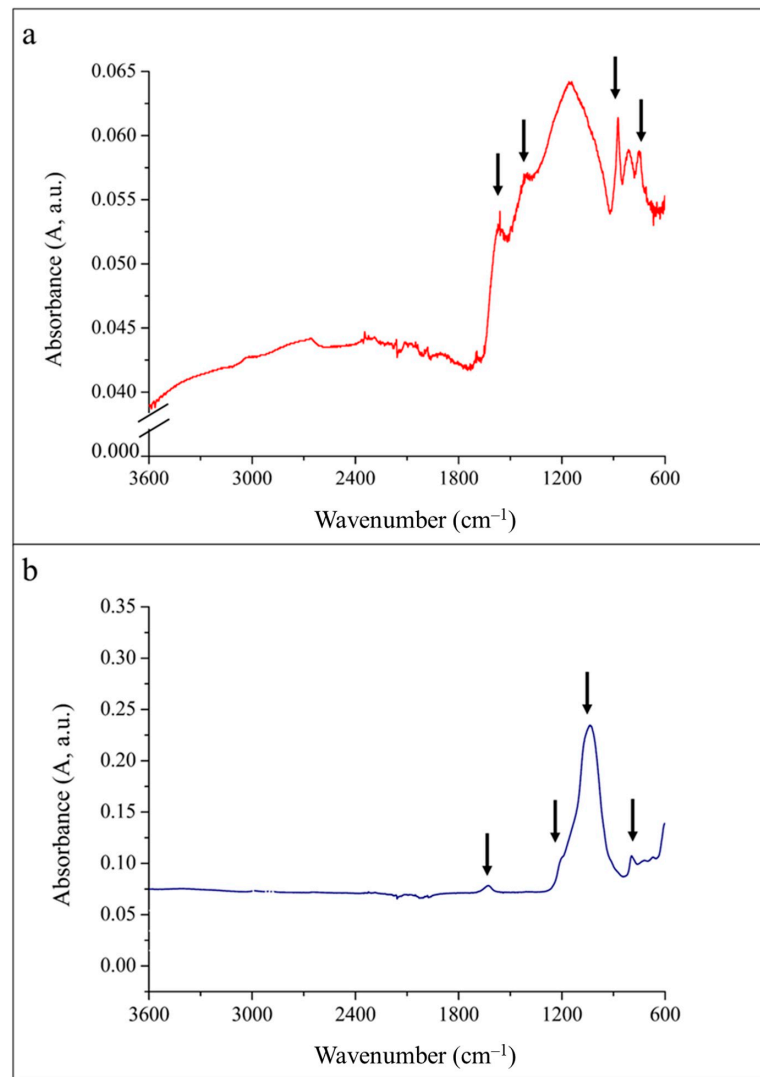


**Figure 4.** ATR-FTIR biochar (a) and zeolite (b) spectra in the range 3600–600 cm<sup>-1</sup> wavenumber.

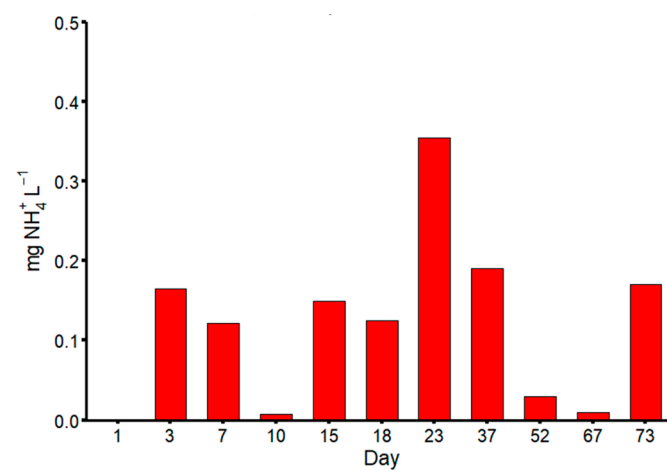


**Figure 5.** NH<sub>4</sub><sup>+</sup> concentration in the influent entering the columns during the experiment.

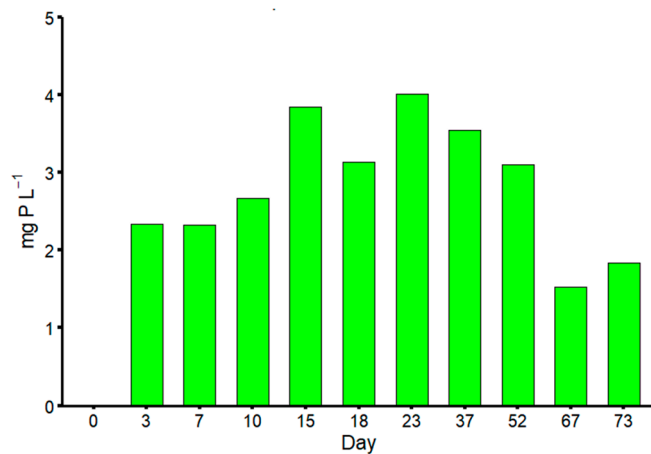


Figure 6. P concentration in the influent entering the columns during the experiment.

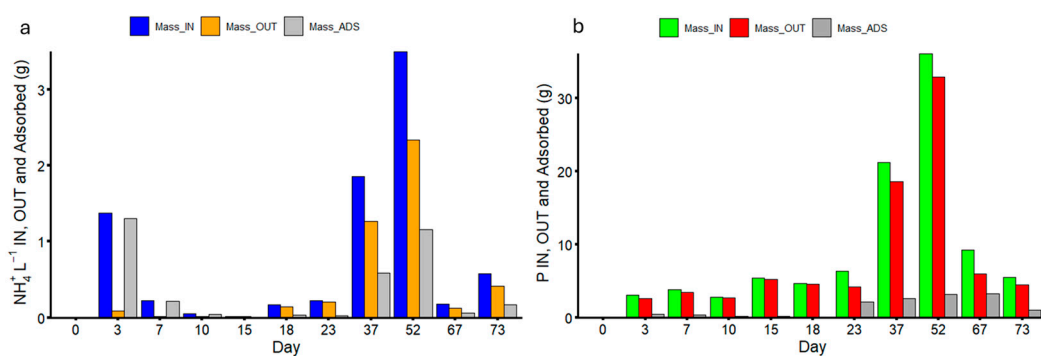


Figure 7. P (a) and NH<sub>4</sub><sup>+</sup> (b) mass balance.

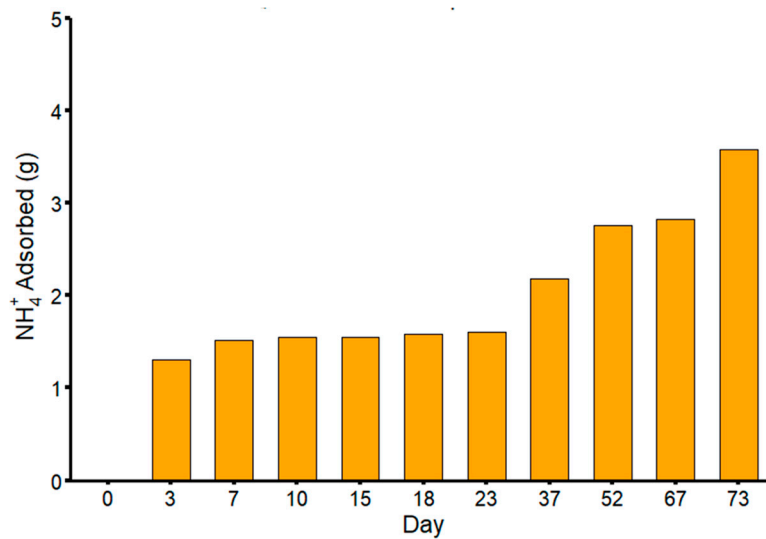
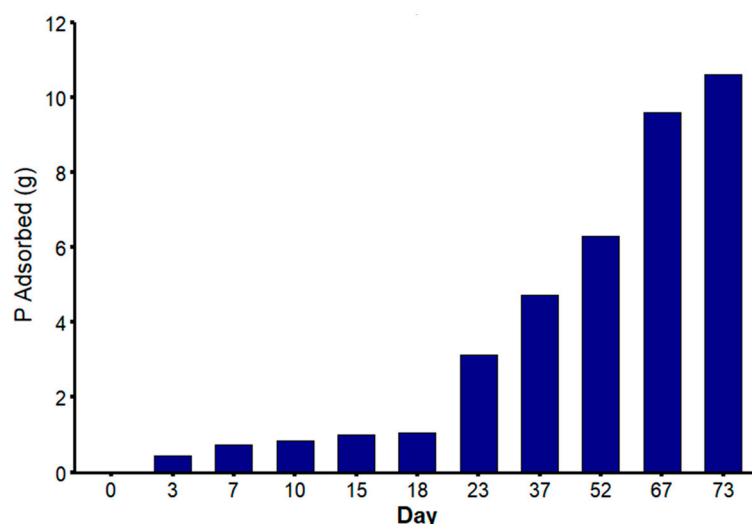


Figure 8. Cumulated mass of NH<sub>4</sub><sup>+</sup> adsorbed by biochar during the 73 test days.



**Figure 9.** Cumulated mass of P adsorbed by zeolite during the 73 test days.

#### 4. Discussion

The higher  $\text{pH}_{\text{pzc}}$  of biochar suggests that its surface remains neutral or positively charged at lower pH levels, making it more favorable for adsorbing negatively charged species like phosphates. However, the maximum adsorption capacity of biochar for P in a mono-component solution was relatively low, at  $0.7 \text{ mg P g}^{-1}$ , likely due to its limited surface area and functional group interactions. Zeolite exhibited a lower  $\text{pH}_{\text{pzc}}$  (6.0), indicating that it acquires a negative charge more readily at slightly acidic pH values. This enhances its ability to attract and adsorb positively charged ions, such as  $\text{NH}_4^+$ , which make zeolite a more efficient material for  $\text{NH}_4^+$  removal from aqueous solutions.

Regarding the analysis of ATR-FTIR spectra, the peaks identified in the ATR-FTIR spectrum of biochar about  $1620 \text{ cm}^{-1}$  indicate O-H stretching vibrations in hydrogen bonded groups and water molecules within the inner layer, as reported by Jung et al. [62] (Figure 4a). Additionally, the peaks at  $1260$  and  $1020 \text{ cm}^{-1}$  suggested the presence of C-O stretching in aromatic components, C=O stretching in conjugated ketones and quinones, and symmetric C-O-C stretching in ester groups found in cellulose and hemicellulose [63]. These components are integral to the aromatic structure of lignin [64]. Another peak identified around  $800 \text{ cm}^{-1}$  is generally associated with bending vibrations of =C-H bonds in aromatic rings.

In the ATR-FTIR spectra analysis, the tested zeolite showed the presence of peaks at  $1650 \text{ cm}^{-1}$  that can be interpreted as resulting from C=O bond stretching or from certain forms of bound water or internal hydroxyl groups (Figure 4b). The spectral regions of  $1250\text{--}950 \text{ cm}^{-1}$  and  $720\text{--}650 \text{ cm}^{-1}$  are characteristic of symmetrical and asymmetrical stretching associated with the internal tetrahedral linkages in the zeolite framework. Furthermore, the  $1100\text{--}1000 \text{ cm}^{-1}$  range typically signifies stretching vibrations of Si-O and Al-O bonds in the siliceous or aluminosiliceous structures of zeolite.

This study was carried out in a real WWTP, and thus, the quality of the effluent is closely related to the characteristics of the incoming wastewater. This explains why N and P concentrations fluctuated during the experimental trial. However, the concentration of  $\text{NH}_4^+$  and P in the WWTP effluent was low; the materials demonstrated an excellent adsorption capacity. Such low N and P concentrations suggest that WWTP efficiently reduces nutrients from wastewater. The low concentrations, particularly of  $\text{NH}_4^+$ , can be partly attributed to the nitrification processes taking place in the biological reactor of the plant [65]. Despite fluctuations in the concentrations of  $\text{NH}_4^+$  and P, zeolite and biochar

performed positively as adsorbents. Some studies in the literature have carried out column studies to evaluate the adsorption capacities of these materials (Table 4).

**Table 4.** Column studies conducted to evaluate the adsorption capacity of zeolite and biochar.

Material	Nutrient Concentration	Type of Solution	Type of Experiment	Reference
Zeolite from volcanic ash	10–40 mg NH <sub>4</sub> <sup>+</sup> L <sup>-1</sup>	Deionized water vs. secondary effluent wastewater	Batch and column	[65]
Natural and modified zeolites	500 mg NH <sub>4</sub> <sup>+</sup> L <sup>-1</sup>	Swine wastewater	Batch and column	[66]
Natural zeolite	263.2–1363.6 mg NH <sub>4</sub> <sup>+</sup> L <sup>-1</sup>	Wastewater	Batch and column	[67]
Natural zeolite	0.2–300 g NH <sub>4</sub> -N m <sup>-3</sup>	Wastewater	Column	[68]
Natural zeolite	60–800 mg NH <sub>4</sub> <sup>+</sup> L <sup>-1</sup>	Wastewater	Column	[69]
Natural zeolite	22 mg NH <sub>4</sub> <sup>+</sup> L <sup>-1</sup>	Wastewater	Column	[49]
Magnesium modified biochar	10 mg PO <sub>4</sub> <sup>3-</sup> L <sup>-1</sup>	Wastewater	Column	[70]
Aluminum modified biochar	25–100 mg PO <sub>4</sub> <sup>3-</sup> L <sup>-1</sup>	Aqueous solution	Column	[71]
Natural biochar	25 mg PO <sub>4</sub> <sup>3-</sup> L <sup>-1</sup>	wastewater	Column	[50]
Calcium modified biochar	2000 mg PO <sub>4</sub> <sup>3-</sup> L <sup>-1</sup>	Aqueous solution	Batch and Column	[62]
Magnesium modified biochar	20–500 mg PO <sub>4</sub> <sup>3-</sup> L <sup>-1</sup>	Water	Batch and Column	[72]

Regarding the zeolite column, the NH<sub>4</sub><sup>+</sup> adsorbed was lower than that reported in previous studies [31,73–75]. This was attributed to the low and fluctuating concentrations of NH<sub>4</sub><sup>+</sup> in the effluents used during the experiment, with an average value of 0.12 mg L<sup>-1</sup>. According to previous batch studies during which the same zeolite was tested for NH<sub>4</sub><sup>+</sup> adsorption, it can be concluded that after 73 days of experiment, zeolite could still adsorb NH<sub>4</sub><sup>+</sup> from treated wastewater. This is due to its unique crystalline structure, which forms molecular-sized cavities and channels, facilitating the entrapping of NH<sub>4</sub><sup>+</sup>, and its high cation exchange capacity, originating from the isomorphic substitution of Si<sup>4+</sup> with Al<sup>3+</sup> [76–78]. Additionally, zeolites can exchange their cations with those in the surrounding environment, such as NH<sub>4</sub><sup>+</sup>, without altering their crystalline structure. The small particle diameter of the zeolite used also facilitated adsorption. Zeolites with smaller particle diameters possess smaller pores and a higher specific surface area [75,79]. This increased specific surface area provides a greater contact area for ions, enhancing the adsorption capacity due to the higher number of available sites for interaction with NH<sub>4</sub><sup>+</sup> ions [80].

Some studies in the literature demonstrate the adsorption capacity of zeolite to NH<sub>4</sub><sup>+</sup>, even if most were made with much higher concentrations of NH<sub>4</sub><sup>+</sup> than those of this study. For example, Nguyen et al. [68] tested the adsorption capacity of a natural zeolite by performing a column study with a flow rate of 15.9 mm min<sup>-1</sup> and a concentration of NH<sub>4</sub><sup>+</sup> in treated wastewater of 100 g m<sup>-3</sup>. The results showed an efficiency in adsorption of about 87%. Another study was conducted by Muscarella et al. [81]. The authors tested the adsorption capacity of NH<sub>4</sub><sup>+</sup> from a natural zeolite TWW, also evaluating the influence of parameters such as particle size and flow rate. The study used two zeolites with different particle diameters (0.5–1.0 and 2.0–5.0 mm) and two flow rates (1.6 and 2.3 L h<sup>-1</sup>). The concentration of NH<sub>4</sub><sup>+</sup> was between 3–21 mg L<sup>-1</sup>. Among the results, the amount of NH<sub>4</sub><sup>+</sup> adsorbed depends exclusively on the quantity of NH<sub>4</sub><sup>+</sup> in contact with the surface of the zeolite. In the study conducted by Zabochnicka-Świątek et al. [82], they used a clinoptilolite zeolite with a particle size of 0.12 mm to test the adsorption capacity of natural clinoptilolite to remove NH<sub>4</sub><sup>+</sup> ions from TWW. The results showed that clinoptilolite can remove up to 99.7% of NH<sub>4</sub><sup>+</sup> ions with a maximum adsorption capacity of 3.8 mg g<sup>-1</sup> for an initial concentration of 300 mg L<sup>-1</sup> of NH<sub>4</sub><sup>+</sup>. The study shows that clinoptilolite has significant potential for treating ammonia-contaminated water, with removal efficiency influenced by initial NH<sub>4</sub><sup>+</sup> concentration and exposure time. These studies align with the test results, where the concentration of NH<sub>4</sub><sup>+</sup> and the contact time between the TWW and the material

play a key role. A recent study carried out in column by Bulacio Fischer et al. [49] evaluated the adsorption capacity of  $\text{NH}_4^+$  by the same zeolite with two different particle sizes (0.5–1.0 mm and 2.0–5.0 mm) tested at three different flow rates (1.2, 1.6 and 2.4 L h<sup>-1</sup>). The results showed that increasing the flow rate improved the adsorption capacity of both zeolites by up to 29% compared with the lowest flow rate. In addition, the zeolite with smaller particles (0.5–1.0 mm) adsorbed about 60 mg more  $\text{NH}_4^+$  than the zeolite with larger particles (2.0–5.0 mm), confirming the influence of size on adsorptive capacity. The desorption phase showed rapid release of  $\text{NH}_4^+$ , with 44–78% of the adsorbed amount released in the first 30 min. Finally, the desorption test conducted with the lowest flow rate achieved the highest  $\text{NH}_4^+$  release, with values 123–148% higher than the highest flow rates.

Regarding the column filled with biochar, the adsorption trend was similarly positive despite some clogging issues. The high P adsorption by woody-feedstock biochar can be attributed to its highly porous structure with a large area available for adsorption. This allows the P to interact and link to the biochar surface. In addition, the alkaline pH and presence of elements such as iron and calcium in biochar increase the capacity to retain P in phosphate. Finally, the biochar used in this study has a highly developed organic matrix with functional groups on the surface (e.g., hydroxyl or carboxyl) that can participate in chemical interactions with phosphates [83,84].

Among the studies carried out to test the adsorption capacity of biochar, a column study using TWW was carried out by Jiang et al. [72]. In this study, the authors used a magnesium-enriched bamboo biochar obtained at different pyrolysis temperatures. At the highest temperature (600 °C), biochar was able to adsorb the most P, approximately 62.2 mg g<sup>-1</sup>. The authors showed that ligand exchange and electrostatic attraction are among the most important characteristics of adsorption. Indeed, the basic pH of the biochar and the increased presence of magnesium due to the enrichment have improved the adsorption capacity of the biochar. Another study was conducted by Muscarella et al. [85] in which three different flow rates (0.7, 1.7 and 2.3 L h<sup>-1</sup>) were tested to evaluate the influence of flow on the adsorption of P from treated TWW. The woody feedstock biochar obtained at a pyrolysis temperature of 500 °C is less, obtaining the greatest adsorption after 7 h in the column with the highest flow rate. In addition to the influence of flow rate, the concentration of P in the TWW also plays a key role, obtaining a higher adsorption rate at times when the concentration of P was higher. This result is in line with the study conducted in our case. The days of the highest P adsorption correspond to the days of the highest P concentration in the effluent. A column study using a similar size column to that used in our case study was carried out by Dalahmeh et al. [86]. The authors examined the effectiveness of biochar, enriched with iron or calcium, as a filter material for phosphate removal from TWW in decentralized wastewater treatment systems (OWTS). The results showed that the biochar enriched with iron had the highest maximum adsorption capacity (3.2 mg g<sup>-1</sup>, according to Langmuir models). After 148 weeks of treatment, the P removal efficiency was 40% for calcium-enriched biochar and 88% for iron-enriched biochar. The analysis of the breakthrough curves indicated that the iron-enriched biochar filter could remain active for 58 months, and the calcium-rich biochar filter could stay active for 15 months at low phosphate concentrations (<2.6 mg L<sup>-1</sup>). These results suggest that biochar enriched with iron and calcium is a promising solution for removing phosphate from TWW in OWTS. The study confirms how the material can continue to adsorb P for long periods, even at low concentrations, and this is in line with the results of our study, which was carried out for 73 consecutive days. A recent study by Januševičius et al. [50] analyzed the adsorption capacities of a biochar obtained from municipal sewage sludge at different temperatures (400, 500 and 600 °C). The properties of biochar, including specific surface area, volume

and pore size distribution, were characterized. The results showed that biochar derived from sewage sludge is a mesoporous material with good adsorptive potential. Although increasing the pyrolysis temperature to 600 °C reduced the specific surface area compared with that obtained at 400 °C, an increase in the surface area of mesopores was observed, thus improving adsorption performance. Two filtration experiments, conducted at a flow rate of 8 mL/min, showed that the column containing biochar pyrolyzed at 600 °C showed the highest phosphorus retention capacity, with retention efficiencies of 87% and 78% in the two consecutive experiments.

Another mechanism that affected P removal was P precipitation since the pH value of wastewater is 7.8 and the  $\text{pH}_{\text{pzc}}$  value of biochar is 5.5. In addition, as it contained calcium, calcium phosphates were also formed and precipitated. For example, Yang et al. [87] noted that as the pH increased, the absorption capacity of iron-modified biochar decreased. The authors attributed such a phenomenon to the increasing concentration of hydroxide ions competing with phosphate for absorption sites. Additionally, the biochar surface becomes negatively charged with increasing pH, leading to intensified electrostatic repulsion between phosphate and biochar, ultimately resulting in poor phosphate adsorption.

It cannot be ignored that the adsorption capacity of biochar was reduced due to some clogging issues that occurred during the experimental trial. In experiments with adsorbents placed in columns, clogging phenomena frequently occur due to suspended solids in effluent. Specifically, aggregations of these suspended solids can be formed within the columns, partially clogging the passage of the effluent and limiting the contact between the adsorbing material and the incoming effluent. This increase can be attributed to a high organic and inorganic load received by the plant compared to its treatment capacity, problems related to reduced sedimentation efficiency in primary or secondary sedimentation tanks, or hydraulic or organic shocks, where sudden changes in hydraulic flow or unexpected organic loads may overload the plant, thereby reducing the removal efficiency of suspended solids [88–91]. However, in view of a future application of adsorbing columns filled with biochar and zeolite at full scale, arranging a filter filled with inert particles (e.g., sand) to hold suspended solids could be useful.

## 5. Conclusions

Zeolite and biochar proved to be suitable for nutrient recovery, showing good adsorption capacity for both P and N. The results indicate that biochar and zeolite can effectively adsorb nutrients. Zeolite adsorbed 1.33 mg g<sup>-1</sup> of NH<sub>4</sub><sup>+</sup> with an adsorption rate of 44%, while biochar adsorbed 26.75 mg g<sup>-1</sup> of P with an adsorption rate of 13%. However, some limitations related to the presence of suspended solids in the effluent and problems related to the low and variable concentrations of NH<sub>4</sub><sup>+</sup> and P in the plant effluent presented themselves. In view of the future application of adsorption columns filled with biochar and zeolite on a large scale, arranging a filter filled with inert particles (e.g., sand) could be useful to retain suspended solids. In addition, using an effluent with a higher and, more importantly, constant concentration of these nutrients could facilitate the enrichment of the materials. The adsorption capacity of these materials is a feasible solution to the increasing scarcity of resources and the high pollution due to the overuse of fertilizers. The use of these adsorbent materials in a nutrient recovery pathway within wastewater treatment systems enables the use of enriched zeolite as a source of N and enriched biochar as a source of P for plants. This strategy supports the environmental sustainability of agricultural productivity from a circular economy perspective.

**Author Contributions:** Conceptualization, G.M. and V.A.L.; methodology, G.M., V.A.L., D.D.T., P.T.B.F. and S.M.M.; formal analysis, D.D.T., P.T.B.F. and S.M.M.; investigation, G.M., V.A.L., D.D.T., P.T.B.F. and S.M.M.; resources, G.M.; data curation, G.M., V.A.L., D.D.T., P.T.B.F. and S.M.M.; writing—original draft preparation, P.T.B.F. and S.M.M.; writing—review and editing, G.M., V.A.L., D.D.T., P.T.B.F. and S.M.M.; supervision, G.M., V.A.L. and D.D.T.; project administration, G.M.; funding acquisition, G.M. All authors have read and agreed to the published version of the manuscript.

**Funding:** This work was funded by the project “Achieving wider uptake of water-smart solutions—WIDER UPTAKE” (grant agreement number: 869283), financed by the European Union’s Horizon 2020 Research and Innovation Programme, Website <https://wideruptake.unipa.it/> (accessed on 11 March 2025) <https://www.sintef.no/projectweb/wider-uptake/> (accessed on 11 March 2025) principal investigator for the University of Palermo Giorgio Mannina. The Unipa project website can be found at: <https://wideruptake.unipa.it/> (accessed on 11 March 2025).

**Data Availability Statement:** The data presented in this study are available upon request from the corresponding author.

**Conflicts of Interest:** The authors declare no conflicts of interest.

## References

1. Patra, A.K.; Coumar, M.V. Sustainable Soil Resource Management for Food and Nutritional Security under Changing Climate Scenario. *Indian J. Agron.* **2023**, *68*, S78–S97.
2. Gatto, A.; Chepeliev, M. Global Food Loss and Waste Estimates Show Increasing Nutritional and Environmental Pressures. *Nat. Food* **2024**, *5*, 136–147. [[CrossRef](#)]
3. Xu, Y.; Jia, J.; Mahmood, H.; Khalid, S. Natural Resource Depletion and Carbon Inequality: An Empirical Insight from Developed and Developing Countries. *Energy Env.* **2024**. [[CrossRef](#)]
4. Abebe, T.G.; Tamtam, M.R.; Abebe, A.A.; Abtemariam, K.A.; Shigut, T.G.; Dejen, Y.A.; Haile, E.G. Growing Use and Impacts of Chemical Fertilizers and Assessing Alternative Organic Fertilizer Sources in Ethiopia. *Appl. Environ. Soil Sci.* **2022**, *2022*, 4738416. [[CrossRef](#)]
5. Maathuis, F.J. Physiological Functions of Mineral Macronutrients. *Curr. Opin. Plant Biol.* **2009**, *12*, 250–258. [[CrossRef](#)] [[PubMed](#)]
6. Tripathi, D.K.; Singh, V.P.; Chauhan, D.K.; Prasad, S.M.; Dubey, N.K. Role of Macronutrients in Plant Growth and Acclimation: Recent Advances and Future Prospective. In *Improvement of Crops in the Era of Climatic Changes: Volume 2*; Springer: New York, NY, USA, 2014; pp. 197–216.
7. Malhotra, H.; Vandana; Sharma, S.; Pandey, R. Phosphorus Nutrition: Plant Growth in Response to Deficiency and Excess. In *Plant Nutrients and Abiotic Stress Tolerance*; Hasanuzzaman, M., Fujita, M., Oku, H., Nahar, K., Hawrylak-Nowak, B., Eds.; Springer: Singapore, 2018; pp. 171–190, ISBN 978-981-10-9044-8.
8. Khan, F.; Siddique, A.B.; Shabala, S.; Zhou, M.; Zhao, C. Phosphorus Plays Key Roles in Regulating Plants’ Physiological Responses to Abiotic Stresses. *Plants* **2023**, *12*, 2861. [[CrossRef](#)]
9. White, P.J.; Brown, P.H. Plant Nutrition for Sustainable Development and Global Health. *Ann. Bot.* **2010**, *105*, 1073–1080. [[CrossRef](#)]
10. Meshalkin, V.; Malyavin, A.; Kostyleva, V.; Ivanova, V.; Burvikova, J. Life Cycle Assessment and Sustainable Development of Mineral Fertilizers Production. *E3S Web Conf.* **2024**, *510*, 02007. [[CrossRef](#)]
11. Wang, J.; Azam, W. Natural Resource Scarcity, Fossil Fuel Energy Consumption, and Total Greenhouse Gas Emissions in Top Emitting Countries. *Geosci. Front.* **2024**, *15*, 101757. [[CrossRef](#)]
12. Ye, Q. Soil Pollution Status, Sources, and Control Methods in China. *Acad. J. Sci. Technol.* **2024**, *9*, 155–161. [[CrossRef](#)]
13. Du, J.; Waite, T.D.; Feng, J.; Lei, Y.; Tang, W. Coupled Electrochemical Methods for Nitrogen and Phosphorus Recovery from Wastewater: A Review. *Environ. Chem. Lett.* **2023**, *21*, 885–909. [[CrossRef](#)]
14. Theregowda, R.B.; González-Mejía, A.M.; Ma, X.; Garland, J. Nutrient Recovery from Municipal Wastewater for Sustainable Food Production Systems: An Alternative to Traditional Fertilizers. *Environ. Eng. Sci.* **2019**, *36*, 833–842. [[CrossRef](#)]
15. Brownlie, W.J.; Sutton, M.A.; Reay, D.S.; Heal, K.V.; Hermann, L.; Kabbe, C.; Spears, B.M. Global Actions for a Sustainable Phosphorus Future. *Nat. Food* **2021**, *2*, 71–74. [[CrossRef](#)]
16. El Wali, M.; Golroudbary, S.R.; Kraslawski, A. Circular Economy for Phosphorus Supply Chain and Its Impact on Social Sustainable Development Goals. *Sci. Total Environ.* **2021**, *777*, 146060. [[CrossRef](#)] [[PubMed](#)]

17. Chowdhury, R.B.; Moore, G.A.; Weatherley, A.J.; Arora, M. Key Sustainability Challenges for the Global Phosphorus Resource, Their Implications for Global Food Security, and Options for Mitigation. *J. Clean. Prod.* **2017**, *140*, 945–963. [[CrossRef](#)]
18. Jakobsson, A.K. The Phosphorus Challenge in International Politics: Geopolitics, Human Security, and the Grey Zone. *Find-Researcher* **2021**.
19. Khan, M.N.; Mohammad, F. Eutrophication: Challenges and Solutions. In *Eutrophication: Causes, Consequences and Control: Volume 2*; Ansari, A.A., Gill, S.S., Eds.; Springer: Dordrecht, The Netherlands, 2014; pp. 1–15, ISBN 978-94-007-7814-6. [[CrossRef](#)]
20. Huang, J.; Xu, C.; Ridoutt, B.G.; Wang, X.; Ren, P. Nitrogen and Phosphorus Losses and Eutrophication Potential Associated with Fertilizer Application to Cropland in China. *J. Clean. Prod.* **2017**, *159*, 171–179. [[CrossRef](#)]
21. Bijay-Singh; Craswell, E. Fertilizers and Nitrate Pollution of Surface and Ground Water: An Increasingly Pervasive Global Problem. *SN Appl. Sci.* **2021**, *3*, 518. [[CrossRef](#)]
22. El-Nahhal, I.Y.; Al-Najar, H.; El-Nahhal, Y. Cations and Anions in Sewage Sludge from Gaza Waste Water Treatment Plant. *Am. J. Anal. Chem.* **2014**, *5*, 655. [[CrossRef](#)]
23. Rahimi, M.H.; Kalantari, N.; Sharifidoost, M.; Kazemi, M. Quality Assessment of Treated Wastewater to Be Reused in Agriculture. *Glob. J. Environ. Sci. Manag.* **2018**, *4*, 217–230. [[CrossRef](#)]
24. Gholipour, M.; Mehrabanjoubani, P.; Abdolzadeh, A.; Raghimi, M.; Seyedkhademi, S.; Karimi, E.; Sadeghipour, H.R. Facilitated Decrease of Anions and Cations in Influent and Effluent of Sewage Treatment Plant by Vetiver Grass (*Chrysopogon zizanioides*): The Uptake of Nitrate, Nitrite, Ammonium, and Phosphate. *Environ. Sci. Pollut. Res.* **2020**, *27*, 21506–21516. [[CrossRef](#)] [[PubMed](#)]
25. Ye, Y.; Ngo, H.H.; Guo, W.; Chang, S.W.; Nguyen, D.D.; Zhang, X.; Zhang, J.; Liang, S. Nutrient Recovery from Wastewater: From Technology to Economy. *Bioresour. Technol. Rep.* **2020**, *11*, 100425. [[CrossRef](#)]
26. Perera, M.K.; Englehardt, J.D.; Dvorak, A.C. Technologies for Recovering Nutrients from Wastewater: A Critical Review. *Environ. Eng. Sci.* **2019**, *36*, 511–529. [[CrossRef](#)]
27. Robles, Á.; Aguado, D.; Barat, R.; Borrás, L.; Bouzas, A.; Giménez, J.B.; Martí, N.; Ribes, J.; Ruano, M.V.; Serralta, J.; et al. New Frontiers from Removal to Recycling of Nitrogen and Phosphorus from Wastewater in the Circular Economy. *Bioresour. Technol.* **2020**, *300*, 122673. [[CrossRef](#)]
28. Witek-Krowiak, A.; Gorazda, K.; Szopa, D.; Trzaska, K.; Moustakas, K.; Chojnacka, K. Phosphorus Recovery from Wastewater and Bio-Based Waste: An Overview. *Bioengineered* **2022**, *13*, 13474–13506. [[CrossRef](#)]
29. Sengupta, S.; Nawaz, T.; Beaudry, J. Nitrogen and Phosphorus Recovery from Wastewater. *Curr. Pollut. Rep.* **2015**, *1*, 155–166. [[CrossRef](#)]
30. Jung, K.-W.; Kim, K.; Jeong, T.-U.; Ahn, K.-H. Influence of Pyrolysis Temperature on Characteristics and Phosphate Adsorption Capability of Biochar Derived from Waste-Marine Macroalgae (*Undaria Pinnatifida* Roots). *Bioresour. Technol.* **2016**, *200*, 1024–1028. [[CrossRef](#)]
31. Muscarella, S.M.; Badalucco, L.; Cano, B.; Laudicina, V.A.; Mannina, G. Ammonium Adsorption, Desorption and Recovery by Acid and Alkaline Treated Zeolite. *Bioresour. Technol.* **2021**, *341*, 125812. [[CrossRef](#)]
32. Günal, A.; Erdogan, B. Ammonia Removal by Natural and Modified Clinoptilolite: Scientific Paper. *J. Serbian Chem. Soc.* **2022**, *87*, 1395–1407. [[CrossRef](#)]
33. Banik, C.; Bakshi, S.; Andersen, D.S.; Laird, D.A.; Smith, R.G.; Brown, R.C. The Role of Biochar and Zeolite in Enhancing Nitrogen and Phosphorus Recovery: A Sustainable Manure Management Technology. *Chem. Eng. J.* **2023**, *456*, 141003. [[CrossRef](#)]
34. Morante-Carballo, F.; Montalván-Burbano, N.; Carrión-Mero, P.; Espinoza-Santos, N. Cation Exchange of Natural Zeolites: Worldwide Research. *Sustainability* **2021**, *13*, 7751. [[CrossRef](#)]
35. Muscarella, S.M.; Badalucco, L.; Laudicina, V.A.; Mannina, G. Chapter 5—Zeolites for the Nutrient Recovery from Wastewater. In *Current Developments in Biotechnology and Bioengineering*; Mannina, G., Pandey, A., Sirohi, R., Eds.; Elsevier: Amsterdam, The Netherlands, 2023; pp. 95–114, ISBN 978-0-323-99920-5.
36. Muscarella, S.M.; Laudicina, V.A.; Badalucco, L.; Conte, P.; Mannina, G. Ammonium Recovery from Synthetic Wastewaters by Using Zeolitic Mixtures: A Desorption Batch-Study. *Water* **2023**, *15*, 3479. [[CrossRef](#)]
37. Ashrafizadeh, S.N.; Khorasani, Z.; Gorjiara, M. Ammonia Removal from Aqueous Solutions by Iranian Natural Zeolite. *Sep. Sci. Technol.* **2008**, *43*, 960–978. [[CrossRef](#)]
38. Karapınar, N. Application of Natural Zeolite for Phosphorus and Ammonium Removal from Aqueous Solutions. *J. Hazard. Mater.* **2009**, *170*, 1186–1191. [[CrossRef](#)]
39. Steiner, C. Considerations in Biochar Characterization. In *SSSA Special Publications*; Guo, M., He, Z., Uchimiya, S.M., Eds.; American Society of Agronomy and Soil Science Society of America: Madison, WI, USA, 2015; pp. 87–100. ISBN 978-0-89118-967-1.
40. Wang, Y.; Qiu, L.P.; Hu, M.F. Magnesium Ammonium Phosphate Crystallization: A Possible Way for Recovery of Phosphorus from Wastewater. *IOP Conf. Ser. Mater. Sci. Eng.* **2018**, *392*, 032032. [[CrossRef](#)]

41. Singh, A.; Singh, A.P.; Purakayastha, T.J. Characterization of Biochar and Their Influence on Microbial Activities and Potassium Availability in an Acid Soil. *Arch. Agron. Soil Sci.* **2019**, *65*, 1302–1315. [\[CrossRef\]](#)
42. Ippolito, J.A.; Spokas, K.A.; Novak, J.M.; Lentz, R.D.; Cantrell, K.B. Biochar Elemental Composition and Factors Influencing Nutrient Retention. In *Biochar for Environmental Management*; Routledge: London, UK, 2015; ISBN 978-0-203-76226-4.
43. Muscarella, S.M.; Badalucco, L.; Laudicina, V.A.; Conte, P.; Mannina, G. Phosphorus Recovery from P-Enriched Solution by Biochar Activated with Chloride Salts. In *Resource Recovery from Wastewater Treatment*; Mannina, G., Cosenza, A., Mineo, A., Eds.; Springer Nature: Cham, Switzerland, 2024; pp. 36–42.
44. Trazzi, P.A.; Leahy, J.J.; Hayes, M.H.B.; Kwapinski, W. Adsorption and Desorption of Phosphate on Biochars. *J. Environ. Chem. Eng.* **2016**, *4*, 37–46. [\[CrossRef\]](#)
45. Huang, Y.; Lee, X.; Grattieri, M.; Yuan, M.; Cai, R.; Macazo, F.C.; Minter, S.D. Modified Biochar for Phosphate Adsorption in Environmentally Relevant Conditions. *Chem. Eng. J.* **2020**, *380*, 122375. [\[CrossRef\]](#)
46. Deng, Y.; Li, M.; Zhang, Z.; Liu, Q.; Jiang, K.; Tian, J.; Zhang, Y.; Ni, F. Comparative Study on Characteristics and Mechanism of Phosphate Adsorption on Mg/Al Modified Biochar. *J. Environ. Chem. Eng.* **2021**, *9*, 105079. [\[CrossRef\]](#)
47. Zhao, S.; Wang, B.; Gao, Q.; Gao, Y.; Liu, S. Adsorption of Phosphorus by Different Biochars. *Spectrosc. Lett.* **2017**, *50*, 73–80. [\[CrossRef\]](#)
48. Mor, S.; Chhoden, K.; Ravindra, K. Application of Agro-Waste Rice Husk Ash for the Removal of Phosphate from the Wastewater. *J. Clean. Prod.* **2016**, *129*, 673–680. [\[CrossRef\]](#)
49. Bulacio Fischer, P.T.; Di Trapani, D.; Laudicina, V.A.; Mineo, A.; Muscarella, S.M.; Mannina, G. Adsorption and Desorption of Ammonium from Treated Wastewater by Zeolite Filled Columns: An Experimental Study at the Water Resource Recovery Facility of Palermo University—Italy. *J. Environ. Manag.* **2025**, *375*, 124241. [\[CrossRef\]](#) [\[PubMed\]](#)
50. Januševičius, T.; Mažeikienė, A.; Stepova, K.; Danila, V.; Paliulis, D. The Removal of Phosphorus from Wastewater Using a Sewage Sludge Biochar: A Column Study. *Water* **2024**, *16*, 1104. [\[CrossRef\]](#)
51. Mannina, G.; Badalucco, L.; Barbara, L.; Cosenza, A.; Di Trapani, D.; Gallo, G.; Laudicina, V.; Marino, G.; Muscarella, S.; Presti, D.; et al. Enhancing a Transition to a Circular Economy in the Water Sector: The EU Project Wider Uptake. *Water* **2021**, *13*, 946. [\[CrossRef\]](#)
52. Muscarella, S.M.; Laudicina, V.A.; Cano, B.; Badalucco, L.; Conte, P.; Mannina, G. Recovering Ammonium by Treated and Untreated Zeolitic Mixtures: A Comprehensive Experimental and Modelling Study. *Microporous Mesoporous Mater.* **2023**, *349*, 112434. [\[CrossRef\]](#)
53. Nasiruddin Khan, M.; Sarwar, A. Determination of Points of Zero Charge of Natural and Treated Adsorbents. *Surf. Rev. Lett.* **2007**, *14*, 461–469. [\[CrossRef\]](#)
54. Vaičiukynienė, D.; Mikelionienė, A.; Baltušnikas, A.; Kantautas, A.; Radzevičius, A. Removal of Ammonium Ion from Aqueous Solutions by Using Unmodified and H<sub>2</sub>O<sub>2</sub>-Modified Zeolitic Waste. *Sci. Rep.* **2020**, *10*, 352. [\[CrossRef\]](#)
55. Sharma, R.K.; Wooten, J.B.; Baliga, V.L.; Lin, X.; Geoffrey Chan, W.; Hajaligol, M.R. Characterization of Chars from Pyrolysis of Lignin. *Fuel* **2004**, *83*, 1469–1482. [\[CrossRef\]](#)
56. Fischer, P.T.B.; Di Trapani, D.; Laudicina, V.A.; Muscarella, S.M.; Mannina, G. Nutrient Recovery from Columns Filled with Zeolite and Biochar: The Case Study of Marineo (ITALY) Wastewater Treatment Plant. In *Resource Recovery from Wastewater Treatment*; Mannina, G., Cosenza, A., Mineo, A., Eds.; Springer Nature: Cham, Switzerland, 2024; pp. 20–25.
57. Kocaturk, N.P. Recovery of Nutrients from Biogas Digestate with Biochar and Clinoptilolite. Ph.D. Thesis, Sustainable Soil Use, Soil Biology, PE&RC, Wageningen University, Wageningen, The Netherlands, 2016. [\[CrossRef\]](#)
58. Canellas-Garriga, J. *Tertiary Ammonium Removal with Zeolites*; Cranfield University: Bedford, UK, 2018.
59. Michalski, R. Ion Chromatography Applications in Wastewater Analysis. *Separations* **2018**, *5*, 16. [\[CrossRef\]](#)
60. Murphy, J.; Riley, J.P. A Modified Single Solution Method for the Determination of Phosphate in Natural Waters. *Anal. Chim. Acta* **1962**, *27*, 31–36. [\[CrossRef\]](#)
61. Mulvaney, R.L. Nitrogen—Inorganic Forms. In *Methods of Soil Analysis*; John Wiley & Sons, Ltd.: Hoboken, NJ, USA, 1996; pp. 1123–1184, ISBN 978-0-89118-866-7.
62. Jung, K.-W.; Jeong, T.-U.; Choi, J.-W.; Ahn, K.-H.; Lee, S.-H. Adsorption of Phosphate from Aqueous Solution Using Electrochemically Modified Biochar Calcium-Alginate Beads: Batch and Fixed-Bed Column Performance. *Bioresour. Technol.* **2017**, *244*, 23–32. [\[CrossRef\]](#) [\[PubMed\]](#)
63. Lucas, E.G.; Izquierdo, C.G.; Fernández, M.T.H. Changes in Humic Fraction Characteristics and Humus-Enzyme Complexes Formation in Semiarid Degraded Soils Restored with Fresh and Composted Urban Wastes. A 5-Year Field Experiment. *J. Soils Sediments* **2018**, *18*, 1376–1388. [\[CrossRef\]](#)
64. Tomin, O.; Yazdani, M.R. Production and Characterization of Porous Magnetic Biochar: Before and after Phosphate Adsorption Insights. *J. Porous Mater.* **2022**, *29*, 849–859. [\[CrossRef\]](#)

65. Gagliano, E.; Sgroi, M.; Falciglia, P.P.; Belviso, C.; Cavalcante, F.; Lettino, A.; Vagliasindi, F.G.A.; Roccaro, P. Removal of Ammonium from Wastewater by Zeolite Synthetized from Volcanic Ash: Batch and Column Tests. *J. Environ. Chem. Eng.* **2022**, *10*, 107539. [[CrossRef](#)]
66. Cyrus, J.S.; Reddy, G.B. Sorption and Desorption of Ammonium by Zeolite: Batch and Column Studies. *J. Environ. Sci. Health Part A* **2011**, *46*, 408–414. [[CrossRef](#)]
67. Aydın Temel, F.; Çağcağ Yolcu, Ö.; Kuleyin, A. A Multilayer Perceptron-Based Prediction of Ammonium Adsorption on Zeolite from Landfill Leachate: Batch and Column Studies. *J. Hazard. Mater.* **2021**, *410*, 124670. [[CrossRef](#)]
68. Nguyen, M.L.; Tanner, C.C. Ammonium Removal from Wastewaters Using Natural New Zealand Zeolites. *N. Z. J. Agric. Res.* **1998**, *41*, 427–446. [[CrossRef](#)]
69. Moreno Sayavedra, S.; Dockx, L.; Sigurnjak, I.; Akyol, Ç.; Meers, E. Post-Treatment of High-Rate Activated Sludge Effluent via Zeolite Adsorption and Recovery of Ammonium-Nitrogen as Alternative Fertilising Products. *Bioresour. Technol.* **2024**, *403*, 130837. [[CrossRef](#)]
70. Chen, D.; Yin, Y.; Xu, Y.; Liu, C. Adsorptive Recycle of Phosphate by MgO-Biochar from Wastewater: Adsorbent Fabrication, Adsorption Site Energy Analysis and Long-Term Column Experiments. *J. Water Process Eng.* **2023**, *51*, 103445. [[CrossRef](#)]
71. Tran, T.C.P.; Nguyen, T.P.; Nguyen, X.C.; Nguyen, X.H.; Nguyen, T.A.H.; Nguyen, T.T.N.; Vo, T.Y.B.; Nguyen, T.H.G.; Nguyen, T.T.H.; Vo, T.D.H.; et al. Adsorptive Removal of Phosphate from Aqueous Solutions Using Low-Cost Modified Biochar-Packed Column: Effect of Operational Parameters and Kinetic Study. *Chemosphere* **2022**, *309*, 136628. [[CrossRef](#)]
72. Jiang, D.; Chu, B.; Amano, Y.; Machida, M. Removal and Recovery of Phosphate from Water by Mg-Laden Biochar: Batch and Column Studies. *Colloids Surf. A Physicochem. Eng. Asp.* **2018**, *558*, 429–437. [[CrossRef](#)]
73. Saltalı, K.; Sarı, A.; Aydın, M. Removal of Ammonium Ion from Aqueous Solution by Natural Turkish (Yıldızeli) Zeolite for Environmental Quality. *J. Hazard. Mater.* **2007**, *141*, 258–263. [[CrossRef](#)]
74. Lin, L.; Lei, Z.; Wang, L.; Liu, X.; Zhang, Y.; Wan, C.; Lee, D.-J.; Tay, J.H. Adsorption Mechanisms of High-Levels of Ammonium onto Natural and NaCl-Modified Zeolites. *Sep. Purif. Technol.* **2013**, *103*, 15–20. [[CrossRef](#)]
75. Taddeo, R.; Prajapati, S.; Lepistö, R. Optimizing Ammonium Adsorption on Natural Zeolite for Wastewaters with High Loads of Ammonium and Solids. *J. Porous Mater.* **2017**, *24*, 1545–1554. [[CrossRef](#)]
76. Lucero, J.M.; Crawford, J.M.; Wolden, C.A.; Carreon, M.A. Tunability of Ammonia Adsorption over NaP Zeolite. *Microporous Mesoporous Mater.* **2021**, *324*, 111288. [[CrossRef](#)]
77. Widiastuti, N.; Wu, H.; Ang, H.M.; Zhang, D. Removal of Ammonium from Greywater Using Natural Zeolite. *Desalination* **2011**, *277*, 15–23. [[CrossRef](#)]
78. Chen, H.-F.; Lin, Y.-J.; Chen, B.-H.; Yoshiyuki, I.; Liou, S.Y.-H.; Huang, R.-T. A Further Investigation of NH<sub>4</sub><sup>+</sup> Removal Mechanisms by Using Natural and Synthetic Zeolites in Different Concentrations and Temperatures. *Minerals* **2018**, *8*, 499. [[CrossRef](#)]
79. Uygur, V.; Çelik, C.Ş.; Sukusu, E. The Effect of Particle Sizes on Ammonium Adsorption Kinetics and Desorption by Natural Zeolites. *Int. J. Agric. Life Sci.* **2019**, *3*, 371–377.
80. He, W.; Gong, H.; Fang, K.; Peng, F.; Wang, K. Revealing the Effect of Preparation Parameters on Zeolite Adsorption Performance for Low and Medium Concentrations of Ammonium. *J. Environ. Sci.* **2019**, *85*, 177–188. [[CrossRef](#)]
81. Muscarella, S.M.; Laudicina, V.A.; Di Trapani, D.; Mannina, G. Recovering Ammonium from Real Treated Wastewater by Zeolite Packed Columns: The Effect of Flow Rate and Particle Diameter. *Sustain. Chem. Pharm.* **2024**, *41*, 101659. [[CrossRef](#)]
82. Zabochnicka, M.; Mali, K. Removal of Ammonia by Clinoptilolite. *Glob. NEST J.* **2010**, *12*, 256–261.
83. Eduah, J.O.; Nartey, E.K.; Abekoe, M.K.; Henriksen, S.W.; Andersen, M.N. Mechanism of Orthophosphate (PO<sub>4</sub>-P) Adsorption onto Different Biochars. *Environ. Technol. Innov.* **2020**, *17*, 100572. [[CrossRef](#)]
84. Liu, Y.; He, Z.; Uchimiya, M. Comparison of Biochar Formation from Various Agricultural By-Products Using FTIR Spectroscopy. *Mod. Appl. Sci.* **2015**, *9*, p246. [[CrossRef](#)]
85. Muscarella, S.M.; Trapani, D.D.; Laudicina, V.A.; Mannina, G. Phosphorus Recovery from Ultrafiltered Membrane Wastewater by Biochar Adsorption Columns: The Effect of Loading Rates. *Heliyon* **2024**, *10*, e34659. [[CrossRef](#)] [[PubMed](#)]
86. Dalahmeh, S.S.; Stenström, Y.; Jebrane, M.; Hylander, L.D.; Daniel, G.; Heinmaa, I. Efficiency of Iron- and Calcium-Impregnated Biochar in Adsorbing Phosphate From Wastewater in Onsite Wastewater Treatment Systems. *Front. Environ. Sci.* **2020**, *8*, 538539. [[CrossRef](#)]
87. Yang, Q.; Wang, X.; Luo, W.; Sun, J.; Xu, Q.; Chen, F.; Zhao, J.; Wang, S.; Yao, F.; Wang, D.; et al. Effectiveness and Mechanisms of Phosphate Adsorption on Iron-Modified Biochars Derived from Waste Activated Sludge. *Bioresour. Technol.* **2018**, *247*, 537–544. [[CrossRef](#)]
88. Chernicharo, A.D.L.; Von Sperling, M. *Biological Wastewater Treatment in Warm Climate Regions*; IWA Publishing: London, UK, 2005; ISBN 978-1-78040-273-4.
89. Von Sperling, M. *Wastewater Characteristics, Treatment and Disposal*; IWA Publishing: London, UK, 2007; ISBN 978-1-84339-161-6.

90. Grady, C.L., Jr.; Daigger, G.T.; Love, N.G.; Filipe, C.D.M. *Biological Wastewater Treatment*, 3rd ed.; CRC Press: Boca Raton, FL, USA, 2011; ISBN 978-1-4200-0963-7. [[CrossRef](#)]
91. Jenkins, D.; Wanner, J. *Activated Sludge: 100 Years and Counting*; Jenkins, D., Wanner, J., Eds.; IWA Publishing: London, UK, 2014; 288p.

**Disclaimer/Publisher's Note:** The statements, opinions and data contained in all publications are solely those of the individual author(s) and contributor(s) and not of MDPI and/or the editor(s). MDPI and/or the editor(s) disclaim responsibility for any injury to people or property resulting from any ideas, methods, instructions or products referred to in the content.